Monolithic integration of high linearity attenuated counter-propagating optical phase-locked loop coherent receiver

A. Bhardwaj, Y. Li, R. Wang, S. Jin, P. Herczfeld, J.E. Bowers and L.A. Coldren

The first monolithically integrated attenuated counter-propagating optical phase-locked loop based coherent receiver is presented. A spurious-free dynamic range of 131.3 dB $Hz^{2/3}$ is measured in the detector shot-noise limit at 100 MHz, which is the highest reported for a single-chip device.

Introduction: Coherent phase modulated RF/photonic links have been proposed [1, 2] to realise high dynamic range analogue optical links, which require the use of an optical phase-locked loop (OPLL) as a linear phase demodulator. Through feedback, the OPLL forces the output phase response of a local optical phase modulator to mirror the phase of an incoming optical signal. Since high loop gain and wide bandwidth are required for efficient phase tracking, the OPLL must have an extremely short loop delay to ensure feedback stability. This can be realised using an attenuated counter-propagating (ACP) configuration [2], which eliminates the phase delays from the optical phase modulators and photodetectors in the OPLL. Integration of the ACP-OPLL on a single chip is necessary so that the propagation delays arising from optical signal routing and the electrical feedback are minimised.

In this Letter, we describe the first monolithically integrated ACP-OPLL PIC on an indium phosphide (InP) material platform. We present preliminary results that demonstrate the highest spurious-free dynamic range (SFDR) reported for a single-chip OPLL coherent receiver.

ACP-OPLL PIC fabrication: The ACP-OPLL PIC uses shallow multi-quantum wells (MQWs) as highly linear phase modulators with low optical propagation loss. The MQW structure consists of 25 lattice-matched 9 nm-thick $In_{0.65}Ga_{0.35}As_{0.76}P_{0.24}$ wells and 6.5 nm-thick $In_{0.8}Ga_{0.2}As_{0.44}P_{0.56}$ barriers [3]. A 2.5 μm-wide deep ridge waveguide is used, where the MQW layers provide waveguiding of the optical mode. High-resistance electrodes (~150 Ω) provide RF attenuation in the 3 mm-long ACP phase modulators that operate in a push–pull configuration. The balanced photodetector pair uses waveguide uni-travelling carrier photodetectors (UTC-PD). A compact 3 dB 2 × 2 multimode interference (MMI) coupler routes light from the ACP phase modulators into the balanced photodetector pair. A feedback path connecting the balanced photodetector pair to the ACP-phase modulator pair is also monolithically integrated on the ACP-OPLL PIC. The total feedback loop delay is ~10 ps. A detailed design of the ACP-OPLL PIC is presented in [4].

The base epitaxial wafer used in the fabrication is designed on a semi-insulating InP substrate, where the layers defining the UTC-photodetectors are grown on top of the phase modulator MQW structure with a 15 nm InP stop-etch layer in between. The modulator MQW structure is grown on top of a 0.85 μm-thick *n*-doped InP layer. Below the *n*-doped InP, a 100 nm-thick *n*-doped quaternary layer is used to make top-side *n*-metal contacts.

Photodetector regions are formed by selectively wet-etching the UTC-PD layers everywhere except in areas that define the UTC-PDs using an SiN_x hard mask. This is followed by regrowth of a 1.9 μm-thick p^+-InP cladding, where the Zn-doping gradually increases from 5×10^{17} to 1×10^{18} cm^{-3}, a 150 nm-thick p^{++}-InGaAs contact layer and a 400 nm-thick InP sacrificial cap layer. The waveguide pattern is first transferred to a 70 nm-thick Cr hard mask, which in turn is used to pattern a 600 nm-thick SiO_2 hard mask. The Cr hard mask is removed and the SiO_2 hard mask is used to etch deep ridge waveguides using Cl_2:H_2:Ar chemistry in an inductively-coupled plasma reactive ion etching (ICP-RIE) system. The etch depth is controlled so that the etch stops ~0.5 μm below the modulator MQW layers and at least 200–300 nm above the *n*-contact layer. The SiO_2 hard mask is removed and a mesa is defined using a SiN_x hard mask that covers the ridge. The remaining *n*-doped InP outside of the mesa is selectively wet-etched to expose the underlying quaternary *n*-contact layer. A scanning electron microscope (SEM) image of a cross-section of the phase modulator waveguide is shown in Fig. 1. This is followed by a deposition and annealing of *n*-metal contacts, which consists of Ni/AuGe/Ni/Au (5 nm/80 nm/20 nm/120 nm) to provide RF loss in the *n*-ACP electrodes.

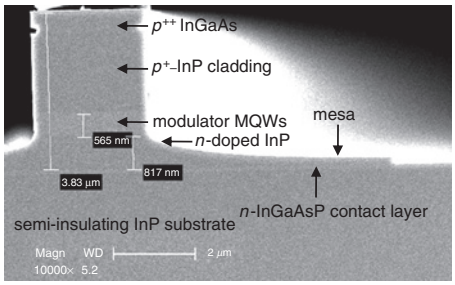

Fig. 1 *SEM image of cross-section of phase modulator waveguide after deep ridge and mesa etch*

Helium implantation is performed to electrically isolate the *n*-contact layers under the different active elements of the ACP-OPLL PIC using a 4.6 μm-thick Ti/Au mask that is defined in two stages using angled electron beam evaporation to prevent voids that would otherwise allow the He^+ ions to reach the semiconductor and block the lateral conduction from the ridge to the *n*-metal contacts. After helium implantation, the Ti/Au mask is removed and a deposition of 200 nm of SiN_x is performed. Proton implantation and subsequent removal of the p^{++}-InGaAs contact layer is performed between the active elements of the ACP-OPLL PIC to increase the electrical isolation in the *p*-doped top cladding layers between them. Proton implantation also reduces the free-carrier-induced optical loss. Photosensitive benzocyclobutene (BCB) is patterned and then hard-cured at 250°C in an N_2 atmosphere. The BCB is patterned on both sides of the ridge waveguides to reduce parasitic capacitance and enable high-speed operation of the 3 mm-long ACP phase modulators. Since the BCB does not planarise equally over the deep ridge waveguides (~3.7 μm tall) with different widths, BCB vias are opened separately over the 2.5 μm-wide ACP modulators and the >10 μm-wide UTC-photodetectors to remove the BCB on top of the ridge waveguides and expose the SiN_x where the *p*-contact vias can be etched later. A deposition of 150 nm-thick SiN_x is done to fill any voids that may have formed between the waveguide sidewalls and BCB. *n*-contact vias are opened over the *n*-contact and *n*-ACP electrodes to enable contact with interconnect metal pads. The SiN_x on top of the ridge is etched using a *p*-contact via, which is designed to be narrower than the waveguide ridge. The sacrificial InP cap layer is selectively wet-etched to expose the p^{++}-InGaAs contact layer. This is followed by deposition and annealing of *p*-metal contacts, which consists of Ti/Pt/Au (20 nm/40 nm/70 nm) to provide the RF loss in the *p*-ACP electrode. A final deposition of Ti/Au (20 nm/1.5 μm) forms pads for electrical contacts and the feedback trace of the OPLL. The wafer is thinned to ~150 μm and back-side metallisation of Ti/Au (20 nm/0.5 μm) is applied. Devices are cleaved and mounted on carriers for testing. Each ACP-OPLL PIC is 4.25 mm long and 350 μm wide and a photograph is shown in Fig. 2.

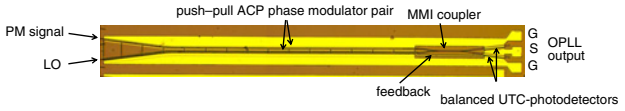

Fig. 2 *Photograph of fully fabricated ACP-OPLL PIC coherent receiver*
PM: phase-modulated

Experiment and results: The phase demodulation linearity of the ACP-OPLL PIC is characterised in a phase modulated optical link at 1550 nm using a low phase noise CW fibre-laser and a $LiNbO_3$ linear phase modulator at the link transmitter. A 250 Ω series resistor is placed between the output of the ACP-OPLL PIC and the external 50 Ω load. This increases the OPLL open-loop gain ensuring adequate voltage drop across the ACP phase modulators. A standard two-tone intermodulation test was performed at 100 MHz. For 12 mA of photocurrent generated in each photodetector, the ACP-OPLL PIC demonstrates a 44.5 dB reduction in the relative nonlinear distortion level with respect to that observed when it operates as a conventional homodyne phase detector without feedback, as shown in Fig. 3.

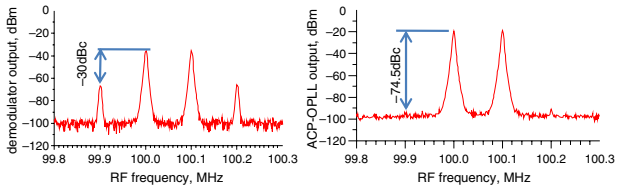

Fig. 3 *Output spectrum showing distortion levels from ACP-OPLL*

a Operating as conventional homodyne phase detector without feedback
b Operating with 12 mA of photocurrent generated in each photodetector
Input RF power is +7 dBm/tone in both cases

The measured fundamental and the nonlinear distortion from the ACP-OPLL PIC are plotted against input RF power in Fig. 4. The distortion level follows a 3:1 slope, indicating that the distortion is due to the third-order nonlinearity. The third-order intermodulation intercept point at the input (IIP3) is +44 dBm. This corresponds to a phase IP3, Φ_{IP3}, of $\sim 7.8\pi$ as the V_π of the phase modulator at the transmitter is 4.5 V. The shot-noise limited link input noise floor (with 12 mA of photocurrent) is −152.6 dBm/Hz. Thus, the measured SFDR is 131.3 dB $Hz^{2/3}$ in the detector shot-noise limit, which is 14 dB higher than the SFDR reported previously in a single-chip OPLL coherent receiver [5].

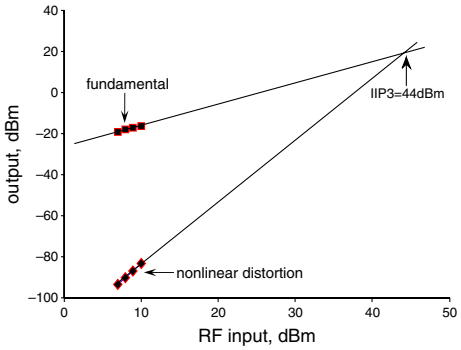

Fig. 4 *Output from ACP-OPLL PIC showing measured fundamental and third-order nonlinear distortion against two-tone RF input power at 100 MHz*

Conclusions: We have presented the first monolithically integrated ACP-OPLL coherent receiver. For 12 mA of photocurrent generated in each photodetector, an SFDR of 131.3 dB $Hz^{2/3}$ is measured in the detector shot-noise limit at 100 MHz, which is the highest SFDR reported in a single-chip OPLL coherent receiver.

Acknowledgment: This work was supported by DARPA under the United States Air Force Contract FA8750-05-C-0265.

25 May 2011
doi: 10.1049/el.2011.1507
One or more of the Figures in this Letter are available in colour online.

A. Bhardwaj, J.E. Bowers and L.A. Coldren (*Department of Electrical and Computer Engineering, University of California, Santa Barbara, CA 93106, USA*)

E-mail: ashish.bhardwaj@jdsu.com

Y. Li, R. Wang and S. Jin (*Department of Electrical and Computer Engineering, University of Massachusetts, Dartmouth, MA 02747, USA*)

P. Herczfeld (*Department of Electrical and Computer Engineering, Drexel University, Philadelphia, PA 19104, USA*)

A. Bhardwaj: Also with JDSU Corporation, 80 Rose Orchard Way, San Jose, CA, 95134, USA

References

1 Chou, H.F., Ramaswamy, A., Zibar, D., Johansson, L.A., Bowers, J.E., Rodwell, M., and Coldren, L.A.: 'Highly linear coherent receiver with feedback', *IEEE Photonics Technol. Lett.*, 2007, **19**, (12), pp. 940–942
2 Li, Y., and Herczfeld, P.: 'Coherent PM optical link employing ACP-PPLL', *J. Lightwave Technol.*, 2009, **27**, (9), pp. 1086–1094
3 Li, Y., Wang, R., Bhardwaj, A., Ristic, S., and Bowers, J.: 'High linearity InP-based phase modulators using a shallow quantum well design', *IEEE Photonics Technol. Lett.*, 2010, **22**, (18), pp. 1340–1342
4 Li, Y., Bhardwaj, A., Wang, R., Jin, S., Coldren, L., Bowers, J., and Herczfeld, P.: 'All-optical ACP-OPLL photonic integrated circuit'. IEEE MTT-S Int. Microw. Symp. Dig., Baltimore, MD, USA, 2011 (paper WE3C-4)
5 Chen, C.H., Ramaswamy, A., Klamkin, J., Johansson, L.A., Bowers, J.E., and Coldren, L.A.: 'Optical phase demodulation using a coherent receiver with an ultra-compact grating beam splitter'. Asia Optical Fiber Communication and Optoelectronic Exp. Conf. (AOE), Shanghai, China, October–November 2008, paper SaN3